Syntaxin clusters assemble reversibly at sites of secretory granules in live cells

S. Barg[a], M. K. Knowles[b], X. Chen[c], M. Midorikawa[c], and Wolfhard Almers[c,1]

[a]Department of Medical Cell Biology, Uppsala University, Uppsala 75123, Sweden; [b]Department of Chemistry and Biochemistry, University of Denver, Denver, CO 80208; and [c]Vollum Institute, Oregon Health and Science University, Portland, OR 97239

Contributed by Wolfhard Almers, October 8, 2010 (sent for review September 17, 2010)

Syntaxin resides in the plasma membrane, where it helps to catalyze membrane fusion during exocytosis. The protein also forms clusters in cell-free and granule-free plasma-membrane sheets. We imaged the interaction between syntaxin and single secretory granules by two-color total internal reflection microscopy in PC12 cells. Syntaxin-GFP assembled in clusters at sites where single granules had docked at the plasma membrane. Clusters were intermittently present at granule sites, as syntaxin molecules assembled and disassembled in a coordinated fashion. Recruitment to granules required the N-terminal domain of syntaxin, but not the entry of syntaxin into SNARE complexes. Clusters facilitated exocytosis and disassembled once exocytosis was complete. Syntaxin cluster formation defines an intermediate step in exocytosis.

molecular docking | dynamic instability | nanodomains | total internal reflection fluorescence

Many interactions between cells require exocytosis. Exocytosis mediates the release of enzymes and messenger substances, and mediates the delivery of membrane proteins into the plasma membrane. During the exocytosis of synaptic vesicles and secretory granules, three so-called SNARE molecules mediate membrane fusion. Syntaxin and SNAP-25 reside in the plasma membrane and a third, VAMP-2/synaptobrevin, resides in the membrane of the vesicle or granule. Biochemical and structural studies have shown that all three combine their SNARE motifs in a *trans*-SNARE complex that bridges the membranes of cells and vesicles/granules. Studies suggest that the energy liberated during the formation of this complex drives membrane fusion (1). The complex recruits also other proteins important for exocytosis (2).

For studies in live cells, electrophysiology has been the method of choice. Electrophysiologic studies have shown that the kinetics of exocytosis change characteristically when SNAREs are disabled by specific proteolytic neurotoxins (3, 4) or replaced with mutated forms (5, 6), and suggest that a "loose" version of the *trans*-SNARE complex forms well before fusion. Electrophysiologic techniques have no rival in terms of temporal resolution, are sensitive enough to detect the exocytosis of single vesicles or granules, and even track the conductance of fusion pores. However, they directly report only membrane fusion, and provide no other signal from secretory vesicles or from the proteins with which a vesicle interacts.

Light microscopy offers an alternative approach. For example, when clathrin-coated vesicles are labeled in one color and a protein such as dynamin in another, it was possible to observe the recruitment and release of dynamin, actin, neural Wiskott Aldrich syndrome protein (7, 8), and other proteins as they collaborate in single endocytic events (9, 10). The approach requires that organelles are separated from neighbors by hundreds of nanometers, such that one may resolve them singly and compare, in the same image, the plasma membrane near the organelle with that further away. Endocrine cells meet this condition, as solitary secretory granules dock at the cell surface and undergo Ca^{2+}-triggered exocytosis (11). Indeed, complexin was recently shown to be transiently recruited to granules during exocytosis (12). Here we explore the relationship between granules and syntaxin clusters.

Results

Syntaxin-GFP Clusters Beneath Secretory Granules. To test whether syntaxin 1A (Syx) in the plasma membrane congregates near docked secretory granules, we imaged PC12 cells coexpressing Syx-GFP and a fluorescent granule marker, neuropeptide-Y (NPY). NPY was fused to the red fluorescent proteins mRFP or mCherry. Because GFP is attached to the extracellular portion of Syx and the red proteins are in granules, neither will disturb the interaction of Syx with other molecules in the cytoplasm. The plasma membrane and the granules adjacent to it were imaged simultaneously in red and green, using total internal reflection fluorescence (TIRF) microscopy. This method selectively imaged a 150-nm thin layer parallel to the cell surface where cells adhered to a glass coverslip. As in previous work (13), the red fluorescence was punctate (Fig. 1 *A* and *B*, *Left*), with each spot representing a secretory granule. When a crippled CMV-promoter ensured low expression levels of Syx-GFP, the green fluorescence was punctate as well (Fig. 1*A* and *B*, *Right*), with each spot representing a cluster of Syx molecules.

To test whether granules recruit Syx, we located granules that appeared round and diffraction-limited and were separated from their nearest neighbor by > 0.58 μm. The minimum distance ensured that all selected granules were surrounded by a zone free of other granules. Nearly half of the qualifying granules (red circles in Fig. 1*B*, *Left*) coincided with Syx clusters (Fig. 1*B*, *Right*), as previously seen in fixed membrane sheets from sonicated cells (14). For example, Fig. 1 *C1* to *C4* were all centered on individual granules. Fig. 1 *C1* and *C3* show the granules themselves, and Fig. 1 *C2* and *C4* the syntaxin images. One of these two granules was associated with a cluster of Syx-GFP molecules.

For analysis, the fluorescence/pixel was measured and averaged over specific regions (e.g., Fig. 1 *C2* and *C4*). "*C*" in Fig. 1*C4* is the Syx fluorescence in a circle centered on a granule (radius, 0.31 μm), and "*S*" in Fig. 1*C4* is that in a concentric annulus (outer radius, 0.49 μm) placed within the granule-free zone. *S* is proportional to the surface density of Syx-GFP molecules in the plasma membrane surrounding the granule. It includes free Syx-GFP and Syx-GFP in granule-unrelated clusters, but not granule-related fluorescence (*SI Text 1* and Fig. S1). The granule-free zone caused a faint, dark ring around the centers of granules and their associated syntaxin clusters, as seen in averaged images printed at high contrast (Fig. 1 *C5* and *C6*). Finally, the difference $\Delta F = C - S$ is the extra fluorescence at the granule site, and is proportional to the number of molecules bound subjacent to the granule. In Fig. 1*C4*, for example, $\Delta F = 104$ camera units (CU). In

Author contributions: S.B., M.K.K., X.C., M.M., and W.A. designed research; S.B., M.K.K., X.C., and M.M. performed research; S.B., M.K.K., X.C., M.M., and W.A. analyzed data; and W.A. wrote the paper.

The authors declare no conflict of interest.

[1]To whom correspondence should be addressed. E-mail: almersw@ohsu.edu.

This article contains supporting information online at www.pnas.org/lookup/suppl/doi:10.1073/pnas.1014823107/-/DCSupplemental.

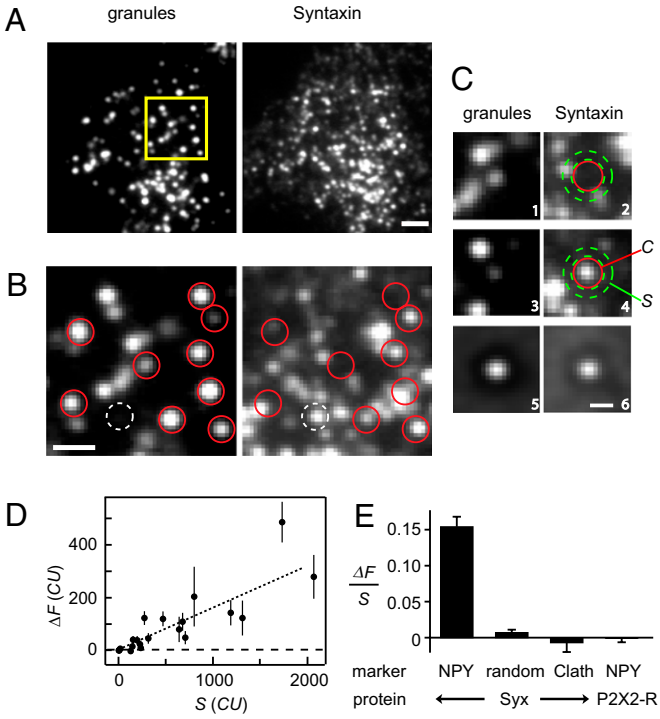

Fig. 1. Syntaxin clusters beneath granules. (*A*) PC12 cell coexpressing NPY-mCherry and Syx-GFP. Same region viewed both in the red (granules) and green (syntaxin) channels. Images are averages of the first 50 frames in a 50-Hz movie. Light exposure 0.1 mJ/ frame, cell MK2316. (Scale bar, 2 μm.) (*B*) Positions of qualifying granules (red) and the position of a Syx-GFP cluster without granule (white) are outlined in enlarged images (yellow in *A*). (Scale bar, 1 μm.) (*C1–C4*) Images centered on two qualifying granules, showing the granules themselves (*C1* and *C3*) and the associated Syx-GFP (*C2* and *C4*). Contrast as in *B*. The variables *C* and *S* were measured in the regions shown in red and green. (*C5* and *C6*) Average of 730 image image pairs (62 cells) as in *C1*, *C2*, and *C3, C4*. (Scale bar, 0.5 μm.) (*D*) $\Delta F = (C - S)$ against the local surface concentration of syntaxin (*S*). Each symbol is an average of 7 to 30 granules in one cell. Values are in camera units (CU) and refer to 0.1 mJ exposures. Coverslip SB2569. (*E*) Extra Syx-GFP detected at granule sites (NPY, average of 62 cells), at random locations in the same cells, or at sites of clathrin-coated pits (Clath, 16 cells). The Clath cells coexpressed Syx-GFP and clathrin light chain-A-conjugated to Ds-Red (7). P_2X_2-receptor-GFP (43) at granule sites was also determined (33 cells). ΔF and *S* were first averaged for each cell as in *D*, and then their ratio was formed. Cells were included if they contained >6 qualifying granules and if $200 < S < 1{,}000$ CU.

a companion article (15), single Syx-GFP molecules were imaged, and their brightness at the excitation energy of Fig. 1 was determined to be $C = 10.4 \pm 0.6$ CU in our 0.31-μm circle. Hence, ΔF in the granule of Fig. 1*C4* represented about 10 fluorescent Syx-GFP molecules.

To assess how well granules and Syx clusters colocalize, we averaged images of each and fitted 2D Gaussians to the results (Fig. 1 *C5* and *C6*). Misalignment would make the SD larger for Syx-GFP than for granules, but they were identical (SD = 125 nm for Syx-GFP and 124 nm for granules). At the light microscopic level, therefore, those granules that were associated with Syx-GFP clusters were precisely aligned with them (*SI Text 2*).

Cells expressing more Syx-GFP in the plasma membrane also had brighter Syx-GFP clusters (Fig. 1*D*). At low expression levels, the relationship between ΔF and *S* was approximately linear. This finding allowed us to use the ratio $\Delta F/S$ to combine results from cells with different expression levels (Fig. 1*E*). There was clear evidence of extra Syx-GFP at granule sites, but not in regions placed randomly onto cells, and not at the sites of clathrin-coated pits. Another plasma membrane protein, a GFP-conjugated P_2X_2 receptor, failed to accumulate near granules (Fig. 1*E*, fourth bar). Apparently, granules specifically accumulate Syx in the subjacent plasma membrane.

On-Granule and Off-Granule Clusters. Most Syx clusters in Fig. 1*B* (e.g., white circle) did not coincide with granules and instead marked unlabeled organelles or no organelles. Such off-granule clusters were previously seen in immunostained and largely (>90%) granule-free plasma membrane sheets from sonicated PC12 cells (16). Given that syntaxin clusters can form anywhere, what targets some of them to granules?

Syntaxin carries a large N-terminal domain (17) that is folded over the SNARE domain in a "closed" form of the protein (18). Both domains participate in binding Munc-18 (19). Because this protein is required for the docking of granules to the plasma membrane (20), we tested three syntaxin mutants defective in binding Munc-18 (Fig. 2*A*). Clustering at granule sites was normal for a mutant unable to assume the closed form [Syx-L165A/E166A (21)], reduced for the SNARE domain mutant Syx-I233A (22) and nearly abolished in a mutant lacking the N-terminal domain [Syx (180-288)-GFP, here called Syx-ΔNT-GFP].

Interestingly, Syx-ΔNT-GFP still congregated in clusters, but the clusters were rarely centered on granules (Fig. 2*B*). To document this point, clusters were located; their positions were copied onto the granule image and scored as to whether they were centered on granules. The fraction of granule-centered clusters was fivefold smaller with Syx-ΔNT-GFP than with Syx-GFP (Fig. 2*C*). Evidently Syx-ΔNT-GFP failed to accumulate significantly beneath granules, even though endogenous Syx presumably still formed clusters there. Therefore, unlike off-granule clusters, on-granule clusters excluded Syx-ΔNT-GFP.

Syx-GFP in Granules Adds Little or No Fluorescence. Synaptic vesicles contain modest amounts of syntaxin (23), possibly because they

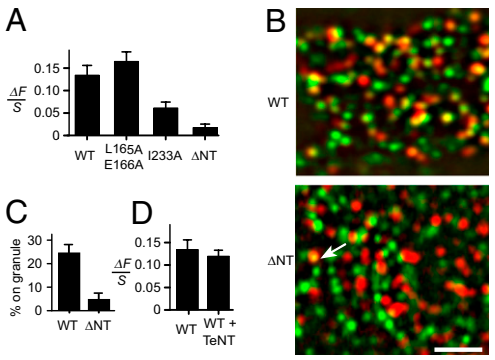

Fig. 2. On-granule clusters exclude a syntaxin mutant. (*A*) Extra fluorescence at granules sites for Syx-GFP (WT, 87 cells) and its mutants. Analysis as in Fig. 1*E*. Cells cotransfected with NPY-mCherry and GFP conjugates of Syx, Syx-L165A/E166A (24 cells), Syx-I233A (19 cells), or Syx-ΔNT (24 cells). (*B*) Cells expressed NPY-mCherry plus either Syx-GFP (WT) or (Syx-ΔNT-GFP (ΔNT). Images were band-pass filtered to enhance punctate fluorescence, then red (granules) and green (Syx-GFP) were merged. In the WT cell many green Syx-GFP clusters colocalized with granules, and in the ΔNT cell only one (arrow). (Scale bar, 2 μm.) (*C*) Percentage of clusters colocalizing with granules. For each cell, 24 to 260 clusters of diffraction-limited size were located in the green image. Circles were centered on them, copied into the red image, and finally scored as to whether or not they were centered on a granule to within 89 nm. Circles placed randomly within the cell outline were scored similarly. The analysis was carried out independently by two observers. The fraction scoring positive was determined both for Syx clusters and for random circles, and the difference is shown ($P < 0.0005$, 15 cells in each group). Granules populated both groups of cells at the same average density (Syx-GFP, 0.99 ± 0.07 /μm^2 and Syx-ΔNT-GFP, 0.95 ± 0.04 /μm^2). (*D*) Extra Syx-GFP as in *A*, compared with cells that expressed in addition TeNT (41 cells).

are recycled from the syntaxin-rich plasma membrane. The granule membrane instead arises through sorting in the Golgi apparatus and is not known to contain syntaxin. Indeed, 44% of granules showed no visible Syx-GFP (Fig. 1*C2*) (15). Do other NPY-positive granules contain syntaxin? The fluorescence of Syx-GFP in such granules would be quenched by the acidic lumen of the granule, and brighten when the intragranular pH is raised. To test this point, cells were first transfected with NPY-mCherry and VAMP-2 conjugated with pHluorin (CMV promoter), a strongly pH-sensitive version of GFP (24). VAMP-2 is the major v-SNARE protein in granules. Each cell was imaged first in buffer, and then again 10 s after 10 mM NH_4Cl had been added (25). When ΔF was measured as in Fig. 1*C*, granule-associated VAMP-2-pHluorin brightened 7.7 ± 1.4-fold (n = 9 cells, 200 < S < 2000 CU). In contrast, granules failed to brighten (by 1.05 ± 0.16-fold, n = 11 cells) when cells expressed Syx-pHluorin instead of VAMP-2-pHluorin. Hence, the granule membrane does not significantly contribute to granule-associated Syx fluorescence.

Lack of Requirement for VAMP-2. Fusion requires *trans*-SNARE complexes, but must Syx molecules enter into such complexes to cluster beneath granules? To address this, cells were cotransfected with Syx-GFP, NPY-mCherry, and the light chain of tetanus neurotoxin (TeNT). TeNT blocks exocytosis by cleaving most of the SNARE motif off VAMP-2 (3), and impairs the entry of the cleaved protein into SNARE complexes (26). TeNT blocked exocytosis in fluorescent PC12-cells as well (Fig. S2) but did not diminish the fluorescence of on-granule clusters (Fig. 2*D*). Apparently the targeting of Syx to granules does not require *trans*-SNARE complexes.

Syx Clusters Increase the Probability of Exocytosis. We next tested whether on-granule Syx clusters are related to exocytosis. Exocytosis of single granules is readily detected when granules are filled with an acid-quenchable fluorescence marker (13, 27). When the fusion pore of a granule opens during exocytosis, hydrogen ions escape, the quenching is relieved, and the granule brightens. Cells were cotransfected with Syx-mCherry and tissue plasminogen activator-GFP (tPA-GFP), a marker that escapes from granules more slowly than NPY-GFP. Fig. 3*A* shows images of a portion of a cell taken while voltage-gated Ca^{2+} channels were opened by raising external $[K^+]$. Exocytosis caused two of the five granules to brighten abruptly and then to dim again as the tPA-GFP was released. Three others remained quiescent. Exocytosis was seen once $[K^+]$ was raised, but not before.

In each cell, we identified all granules (criteria as in Fig. 1) undergoing exocytosis (called responders) and an equal number of other, randomly chosen granules that did not (nonresponders). Each responder was paired with a nonresponder, and for both members of the pair, a common time origin was defined as the last frame before the fluorescence in the responder increased. The procedure allowed us to combine results from responders and nonresponders into two average curves, even though exocytosis occurred at different times in different granules. Responders showed an abrupt increase in fluorescence during exocytosis, whereas nonresponders of course showed no change (Fig. 3*B*).

The fluorescence of Syx-mCherry was measured at the same times and locations as that of the granules. Over the last 9 s before exocytosis, on-granule Syx was brighter in responders ($\Delta F/S$ = 0.072 ± 0.013, n = 148 granules in 13 cells) than in cognate nonresponders ($\Delta F/S$ = 0.033 ± 0.013). The result does not exclude that granules with dim clusters can undergo exocytosis. As few as eight Syx molecules can suffice for exocytosis (cited in ref. 15), and we do not expect to have detected that few in individual granules. Nonetheless, the difference (P < 0.05, paired t test) shows that granules with a Syx cluster were favored for exocytosis over those without.

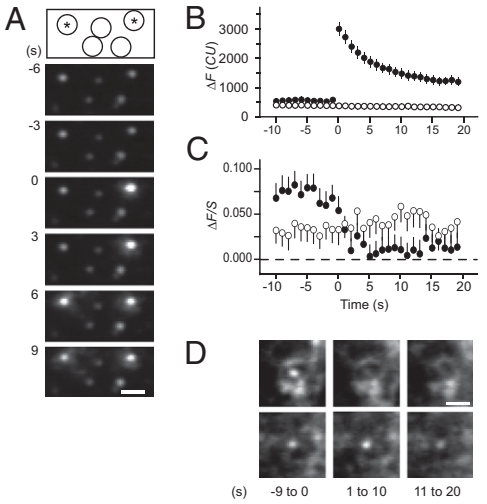

Fig. 3. Syx clusters facilitate exocytosis. (*A*) Sequential images of tPA-GFP in granules. Pairs of 100-ms exposures were given once a second, with the first of the pair at 488 nm to excite tPA-GFP, and the second at 568 nm to excite Syx-mCherry. Drawing on top shows the locations of two granules that brightened (responders, indicated by asterisk) and of three others that did not (nonresponders). Times are relative to the fusion of the granule on the right. Cell SB2652. (Scale bar, 1 μm.) (*B*) Filled circles: tPA-GFP fluorescence recordings of responders were each aligned to the time just before brightening and then averaged. Open circles: recordings from an equal number of nonresponders, aligned to the same times; 148 granules in 16 cells. (*C*) Syx-mCherry fluorescence measured at the same locations and times as the granules in *B*. Filled circles: responders; open circles: nonresponders. Ordinate $\Delta F/S$ as in Fig. 2*A*, except that fluorescence was measured in 0.89-μm diameter circles and in concentric annuli of 0.89 μm inner and 2.4 μm outer diameters. The larger regions help explain why the extra fluorescence, when averaged over responders and nonresponders, is initially smaller than in Fig. 1*E*. (*D*) Syx-mCherry in 13 responders (*Upper*) and 13 nonresponders (*Lower*) from the cell in *A*. Shown are averages over the times shown in seconds beneath each image. In the upper panels, the fluorescence in the center all but vanished. (Scale bar, 1 μm.)

The Syx-mCherry signal essentially vanished after exocytosis, but no similarly large change occurred for nonresponders (Fig. 3*C*). Presumably, Syx emigrated from granule sites by diffusing in the plane of the membrane (15). Averaged images of responders and nonresponders in one cell are shown in Fig. 3*D*.

Syx Clusters Assemble and Disassemble at Stationary Nanodomains. Most granules appear motionless for tens of seconds (28). In the majority of cells, however, Syx clusters seemed surprisingly dynamic even in absence of exocytosis (Movie S1), as long as expression levels were low to moderate (S < 1,000 CU). This impression arose largely because both on- and off-granule clusters disappeared and reappeared at stationary sites (Fig. 4*A*). For analysis, we selected stationary granules bearing detectable Syx-GFP for least 1 s during 50-s movies (Fig. 4 *B* and *C*). In each movie we first identified the image where the cluster was dimmest (*m* image), then examined the periods before and after to find the two images (*b*- and *a*-images, respectively) where the cluster was brightest. Averages of *b, m*, and *a* images confirmed that Syx-GFP clusters essentially vanished and later returned, but the associated granules remained in place throughout (Fig. 4*C*, *Right*). Clusters had ΔF = 114 ± 12 CU in the *b* images, dimmed to 11 ± 7 CU in the *m* images, and recovered to 91 ± 13 CU in the *a* images (n = 81 granules in 10 cells). These values correspond to 11 ± 1 fluorescent molecules in the *b* images, 1 ± 1 molecules in the *m* images, and 9 ± 1 in the *a* images.

Do similar fluctuations also occur with endogenous Syx? A cluster harboring a single fluorescent Syx-GFP molecule will seem

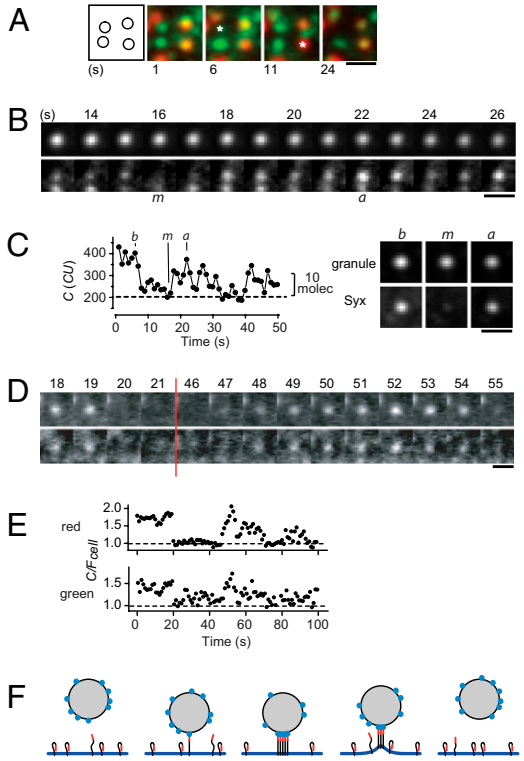

Fig. 4. Clusters spontaneously disassemble and reassemble. (*A*) Portion of a cell showing Syx-GFP (green) and NPY-Cherry fluorescence (red). Averages of consecutive 10 images in a 5-Hz movie (0.1 mJ per exposure at 488 nm); time marked beneath each average. Asterisks show where Syx temporarily disappeared; the rightmost asterisk indicates a granule site. Leftmost panel is a map of Syx-GFP clusters; Cell SB3186. (Scale bar, 1 μm in *A–D*.) (*B*) As in *A*, but with granule (*Upper*) and Syx-GFP (*Lower*) shown separately. Times are relative to beginning of the recording. The letters *m* and *a* mark frames where Syx-GFP was first at a minimum and then at a maximum, respectively. Granule SB3190-08. (*C*) (*Left*) Syx-GFP beneath granule in *B*. Dotted line is the signal during the *m* image and estimates granule-unrelated fluorescence. Letters *b, m,* and *a* mark the times when Syx GFP is at its first maximum (*b*), at its minimum (*m*), and at a second maximum (*a*). (*Right*) Images *b, m,* and *a* were identified for other granules and then averaged (54 granules in five cells). (*D*) Syx clusters in a cell coexpressing Syx-mCherry (*Upper*) and Syx-GFP (*Lower*). Time-lapse at 1 Hz, 0.2 s exposures at 0.04 mJ at both 488 and 568 nm. Times in *s* as in *B*. Granule positions unknown. Cell XC 105e1. (*E*) Red and green fluorescence of the cluster in *D*. Clusters showing fluctuations were located in the red and copied into the green channel; both channels were read out. To correct for bleaching, *C* values were divided by F_{cell}, the fluorescence averaged over the entire footprint of the cell. F_{cell} was measured in an irregular outline drawn to enclose all granules. Correlation between red and green fluorescence was scored by regression analysis in a *t* test (47). (*F*) Granule (shaded), the plasma membrane and Syx molecules with their N terminals in red. "Open" and "closed" forms of Syx are assumed to be in equilibrium. With plasma and granule membranes in proximity, open Syx binds to a ligand on the granule membrane (blue) and assembles into a cluster. When the two membranes separate, the bond is broken and the cluster disassembles.

to empty and refill when that molecule is lost and regained, even if dozens of endogenous molecules remain in place. However, among the 10 fluorescent molecules present initially in *b* images, only one remained in the *m* images. The transient absence of nearly all Syx molecules in a cluster is statistically unlikely unless the behavior of individual molecules is coordinated.

Coordination was confirmed in cells coexpressing Syx-mCherry and Syx-GFP. Red and green Syx disappeared and reappeared at the same time (Fig. 4 *D* and *E*). Their fluorescence was strongly correlated ($P < 10^{-6}$) in 27% of clusters observed (63 clusters from eight cells). In contrast, when each cluster was reanalyzed by comparing its red fluorescence with the green fluorescence of another cluster, a correlation was rarely observed (3%). Apparently, red and green Syx fluorescence vary coordinately in at least some clusters. If the amount of Syx-mCherry in a cluster correlates with that of Syx-GFP, then so, presumably, does the amount of unlabeled Syx. Coordinated variation is expected, for example, when the approach or retreat of a granule causes clusters to assemble and disassemble (Fig. 4*F*).

The time resolution of our movies was more fully exploited to explore faster fluctuations in Fig. 4*C* in detail. Traces from individual on-granule clusters were aligned to the moment when Syx-GFP was at its maximum, and then averaged (Fig. 5*A*, *Upper*). The decline of the curve is taken to represent the lessening chance that a given fluorescent Syx molecule remains in the center, and reflects the exchange of both granule-related and unrelated syntaxin molecules. The initial maximum was diminished or absent when all traces were aligned to the same time, or when cells were fixed and Syx was less mobile (Fig. 5*B*). Apparently, much of the syntaxin subjacent to a granule exchanged within a few seconds, somewhat faster than the assembly-disassembly cycles in Fig. 5 *B* and *D*. The finding suggests that, even during their ~10-s short lifetimes, clusters exchange Syx-GFP with the plasma membrane.

Discussion

By imaging the cell surface of cultured endocrine cells, we have shown that Syx forms clusters at sites precisely aligned with secretory granules. Syx also forms clusters at sites where there are no granules. Such off-granule clusters have been extensively studied in immunostained membrane sheets of sonicated cells. The off-granule clusters were found to form by the homomeric association of Syx SNARE motifs (29, 30). On-granule clusters, in contrast, require the Syx N-terminal domain. Their presence shows that the associated granules have molecularly docked at the plasma membrane. Inasmuch as docking is a prerequisite for fusion, granules with Syx clusters will be favored for exocytosis, as we observed.

Syx clusters formed reversibly at granule sites, hence Syx bound reversibly to a ligand associated with granules; it probably does so in a complex with SNAP-25 (15, 31). What is this ligand? Several candidates may be considered, but none are likely to suffice, at least not on their own. Munc-18 is required for docking (20) along with Syx (32–34), but Munc-18 is not known to associate with granules independently of Syx/SNAP-25, and L165A/E166A, a Syx mutant that does not bind Munc-18 (21), was recruited to granules in normal amounts. The granule membrane protein VAMP-2 binds to Syx via its SNARE motif, but on-granule clusters form also in cells where cleavage of synaptobrevin is expected to prevent *trans*-SNARE complexes to connect granules with the plasma membrane. The granule membrane protein Synaptotagmin-1 participates in granule docking (35). Nonetheless, the Syx mutant

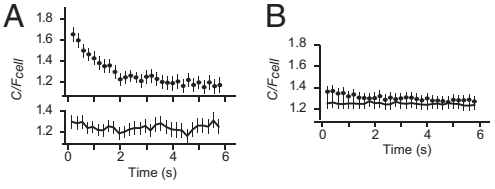

Fig. 5. Rapid Syx fluctuations. (*A*) As in Fig. 4 *B* and *C*, but each frame in 5-Hz movies was analyzed separately and corrected for bleaching, as in Fig. 4*E*. (*Upper*) Traces were first aligned temporally to the time of maximal C/F_{cell} (analogous to the *b* image), and then averaged. (*Lower*) As in *Upper* image, but aligned to the fixed time 10 s after start of illumination. Sixty granules in five cells. Granules were selected to have a strong Syx-GFP signal hence $C/F_{cell} > 1$. (*B*) As in *A*, but from cells fixed in 2% paraformaldehyde (10 min). We excluded granules with the dimmest average Syx fluorescence to match the final value of C/F_{cell} to that in *A*. Ninety-two granules in five cells.

Syx-ΔNT was excluded from on-granule clusters, although Syx-ΔNT retains the SNARE domain, which is the only known synaptotagmin binding site on Syx (36, 37). Finally, the protein CAPS is required for fusion in PC12 cells and binds Syx (38), but its binding partner on granules is unknown. Probably several molecules collaborate in causing Syx to cluster beneath granules. These molecules may also include tethering factors that are functionally similar to p115 in Golgi vesicles (39) or to EEA1, which enters large complexes with Syx during endosome fusion (40).

Surprisingly, Syx molecules in clusters assembled and disassembled in a coordinated fashion, although the associated granule remained in place. Either granules approached and retreated from the plasma membrane over distances too small to detect in our TIRF measurements, or there were biochemical changes that were coordinated at the level of a granule or a cluster. In addition, Syx clusters disassembled in seconds after the exocytosis of the associated granule, even though the remnants of the secretory granule, particularly its membranous cavity, remained in place (11). Syx clusters seem much more dynamic than presynaptic active zones in neurons, where multiple vesicles dock and fuse in succession. Stable active zones are no detriment to exocytic membrane fusion in presynaptic terminals, and it is not obvious physiologically why Syx clusters need to be unstable. Perhaps stable clusters would hinder the dispersion of the *cis*-SNARE complexes generated by exocytosis.

Materials and Methods

Cells. PC12-GR5 cells were maintained in T80 flasks (Nalgene or Nunc) at 37 °C/5% CO_2 in DMEM supplemented with 5% FCS, 5% horse serum, 100 μg/mL penicillin, and 100 μg/mL streptomycin. For microscopy, the cells were plated on poly-L-lysine (Sigma) coated glass coverslips, and transfected 1 to 4 h after plating, by adding plasmid DNA and Lipofectamine-2000 (Invitrogen) to a volume of 1.5 mL, as in the manufacturer's protocol. The amount of DNA was 0.5 to 1.5 μg for fluorescent SNAREs and 0.5 μg for the granule markers NPY-mCherry and tPA-GFP. Imaging started 20 to 30 h after transfection in a buffer containing (in millimolars) 140 NaCl, 3 KCl, 1 $MgCl_2$, 3 $CaCl_2$, 10 D-glucose, 10 hepes, pH 7.4. Temperatures were 37 °C for culture and 28 °C for imaging.

Plasmids. GFP refers to the construct also known as EGFP. The constructs used for mammalian expression of neuropeptide Y-mRFP (11), clathrin light chain α-DsRed (7), tPA-GFP (41), and syntaxin 1A-mRFP (42) have been described. Syntaxin1A-GFP and P_2X_2 receptor-GFP (43) were kind gifts of J. W. Taraska (National Heart, Lung, and Blood Institute, National Institutes of Health, Bethesda) and B. Khakh (Department of Physiology, University of California, Los Angeles), respectively. Syntaxin(180-288)-GFP, hereafter called Syx-ΔNT-GFP, was made by replacing mRFP with GFP in syntaxin-TMD-H3 (42). Syntaxin L165A/E166A was obtained by PCR using the primers ccacgaccagtgaggaagcggcagacatgctggagagtgg and ccactctccagcatgtctgccgcttcctcactggtcgtgg. The I233A mutation was obtained similarly using the primers ggggagatgattgacagggccgagtacaatgtggaacacg and cgtgttccacattgtactcggccctgtcaatcatctcccc. The red fluorescent protein mCherry was amplified by PCR from a prokaryotic expression vector kindly supplied by R. Y. Tsien (Department of Chemistry and Biochemistry, University of California, San Diego) (44), and NPY-mCherry was obtained by replacing GFP using Age1/BsrG1 sites. Syntaxin-pHluorin was made by replacing GFP with pHluorin, and VAMP-2-pHluorin was a gift of D. de Angelis (Memorial Sloan–Kettering Cancer Center, New York) (24). Tetanus toxin light chain was a gift of W. S. Trimble (Program in Neurosciences and Mental Health, The Hospital for Sick Children, Toronto) (45).

To obtain low expression levels of Syx-GFP, we used a truncated CMV promoter, dCMV, that lacks 450 bp in the enhancer region (46), which was obtained by replacing the CMV sequence with the corresponding sequence from dCMV-vinculin (a kind gift of C. Waterman-Storer, National Heart, Lung, and Blood Institute, National Institutes of Health, Bethesda) using Ase1/Nhe1. Promoter and complete coding regions of all plasmids were nucleotide sequenced for verification.

Fluorescence Microscopy. The plasma membrane and its associated granules were illuminated by TIRF and viewed on an Olympus IX 70 microscope, as described (13), and using a 1.45 N.A. objective (Apo 60×; Olympus). GFP was excited at 488 nm and mCherry (or mRFP) at 568 nm; both wavelengths were present simultaneously, unless specified. An acousto-optical tunable filter (Neos) selected the laser wavelength, controlled its power and turned the light on and off. The beam passed through a double band-pass filter (488/568; Chroma) and a spatial filter, and was then directed into the objective with a dual-band dichroic mirror reflecting from 466 to 498 nm and from 554 to 589 nm. The beam left the objective at an angle of 66 to 67.7°, as determined by replacing the glass coverslip with a hemispherical prism of the same refractive index. In a medium of refractive index 1.37, this would produce an evanescent field declining *e*-fold over 171 to 123 nm.

The illumination intensity near the glass-cell interface depends both on the power of the incident light and on the angle at which the light enters the coverslip. That angle was reproduced from day to day by imaging beads at a laser-power of 50 μW (488 nm, average of 50 exposures of 20 ms), finding their locations in the image with Metamorph's Find Spots application and then measuring their green fluorescence (see below). Results were averaged for all 100 to 200 beads each in a total of five to eight images. If the average differed by more than 15% from a reference reading (4,820 CU), the position of the beam in the back focal plane was adjusted and the procedure repeated. Once the beads fluoresced at about 4,820 units at 50 μW, the power at 488 nm was increased to levels as indicated.

Red and green fluorescence were separated with an image splitter (DualView; Optical Insights) containing a dichroic mirror (565 nm), a green band-pass filter (500–550 nm) and a red long-pass filter (585 nm, all from Chroma). A slight difference in focus between red and green images was canceled by inserting a lens of 400-mm focal length in the red emission path. Red and green images were projected side-by-side onto a back-illuminated EMCCD camera (Cascade 512B; Roper Scientific). Each image covered a 22 × 22-μm square in the center of the field of view. Image magnification was 180× and provided 89 nm/pixel on the camera chip. The alignment of the red and green images was determined once every experimental session by imaging yellow-green fluorescing 200-nm beads (Molecular Probes) that were stuck on the coverslip. An algorithm programmed in MATLAB (25) was used to shift and shrink (by <4%) the red image until each bead therein superimposed on its location in the green image. Images were acquired at 120× electron multiplication gain and unity digital gain, and pixels read out at 10 MHz. For direct viewing during an experiment, each eyepiece was fitted with a dual-emission filter. Unless indicated otherwise, movies were taken in "stream" mode and the acquisition frequency was the inverse of the exposure time. In Figs. 1 and 2, most streams were immediately averaged into single images.

Cells were found by exciting the granules (marked with NPY-mRFP or NPY-mCherry) at 568 nm only, and once the granules were in focus, an 488 nm excitation applied as well. Excitation intensities at 488 nm varied inversely with the duration over which we wished to record, with the exposure duration adjusted to deliver a light energy of 0.1 mJ per exposure. In single-molecule measurements only, the light energy was 1 mJ per exposure.

Analysis and Definitions. Fluorescence intensities (called fluorescence) were measured in regions of interest as the average fluorescence per pixel using the Metamorph Region Measurements Average Intensity command, and are given in camera units. Most images showed only one cell. The average "off-cell" fluorescence was measured in regions outside the footprint of cells and subtracted. Background-subtracted measurements are denoted by the variable *F*.

Specifically, *F* was called *C* when averaged over Metamorph circles of 7 pixel in diameter (0.312 μm in radius). Circles were centered at the locations of solitary granules or, more rarely, of syntaxin clusters, and were placed by eye to within one pixel (89 nm). Usually the fluorescence was determined also in a concentric annulus surrounding the circle; its inner and outer radii were 0.31 and 0.49 μm, respectively. The *F* value in the annulus is called *S* (for "surround"). The difference $(C - S)$ is called ΔF.

During analysis, the granule image was viewed first to find suitable granules. Such granules appeared diffraction-limited and round, were not located at the edge of the cell, and separated from their neighbors by >0.58 μm. The minimum distance ensured that all chosen granules were surrounded by a granule-free zone. In some cells, granules were so closely packed that fewer than seven qualified for analysis; such cells were not analyzed. Circles of 0.31-μm radius were centered on granules (usually the red image) and then duplicated into the Syx image (usually green). All later steps in the analysis were carried out automatically using Metamorph journal functions and Excel.

When analyzing regions placed at random on cells, the cell outline was first determined by locating the granules with the Metamorph Find Spots application, and then drawing the smallest outline that contained all granules. Next, the outline was copied into the Syx channel and populated with randomly placed circle/annulus combinations at a density of about $1/\mu m^2$.

We corrected for the possibility that dim green fluorescence might result from immature mCherry. Cells expressing only NPY-mCherry were excited simultaneously with 488 nm (5 mW) and 568 nm (5 mW) light. As a fraction of the red signal, the green "signal" was $0.5 \pm 0.2\%$ (393 granules in five cells).

Throughout, results are given ± SE of mean and significance is assessed in *t* tests.

ACKNOWLEDGMENTS. We thank Manfred Lindau, Ling-Gang Wu, Justin Taraska, Thorsten Lang, Bertil Hille, Steve Arch, Erik Gylfe, and Volker Gerke for their helpful suggestions on the manuscript. This study was supported in part by the Knut and Alice Wallenberg foundation (S.B.), a European Molecular Biology Organization long-term fellowship (to S.B.), National Research Service Award fellowship DK074292 (to M.K.K.), and National Institutes of Health Grant MH060600 (to W.A.).

1. Jahn R, Lang T, Südhof TC (2003) Membrane fusion. *Cell* 112:519–533.
2. Südhof TC, Rothman JE (2009) Membrane fusion: Grappling with SNARE and SM proteins. *Science* 323:474–477.
3. Xu T, Binz T, Niemann H, Neher E (1998) Multiple kinetic components of exocytosis distinguished by neurotoxin sensitivity. *Nat Neurosci* 1(3):192–200.
4. Sakaba T, Stein A, Jahn R, Neher E (2005) Distinct kinetic changes in neurotransmitter release after SNARE protein cleavage. *Science* 309:491–494.
5. Sørensen JB, et al. (2006) Sequential N- to C-terminal SNARE complex assembly drives priming and fusion of secretory vesicles. *EMBO J* 25:955–966.
6. Kesavan J, Borisovska M, Bruns D (2007) v-SNARE actions during Ca(2+)-triggered exocytosis. *Cell* 131:351–363.
7. Merrifield CJ, Feldman ME, Wan L, Almers W (2002) Imaging actin and dynamin recruitment during invagination of single clathrin-coated pits. *Nat Cell Biol* 4:691–698.
8. Merrifield CJ, Qualmann B, Kessels MM, Almers W (2004) Neural Wiskott Aldrich Syndrome Protein (N-WASP) and the Arp2/3 complex are recruited to sites of clathrin-mediated endocytosis in cultured fibroblasts. *Eur J Cell Biol* 83(1):13–18.
9. Ehrlich M, et al. (2004) Endocytosis by random initiation and stabilization of clathrin-coated pits. *Cell* 118:591–605.
10. Yarar D, Waterman-Storer CM, Schmid SL (2005) A dynamic actin cytoskeleton functions at multiple stages of clathrin-mediated endocytosis. *Mol Biol Cell* 16: 964–975.
11. Taraska JW, Almers W (2004) Bilayers merge even when exocytosis is transient. *Proc Natl Acad Sci USA* 101:8780–8785.
12. An SJ, Grabner CP, Zenisek D (2010) Real-time visualization of complexin during single exocytic events. *Nat Neurosci* 13:577–583.
13. Taraska JW, Perrais D, Ohara-Imaizumi M, Nagamatsu S, Almers W (2003) Secretory granules are recaptured largely intact after stimulated exocytosis in cultured endocrine cells. *Proc Natl Acad Sci USA* 100:2070–2075.
14. Lang T, et al. (2001) SNAREs are concentrated in cholesterol-dependent clusters that define docking and fusion sites for exocytosis. *EMBO J* 20:2202–2213.
15. Knowles MK, et al. (2010) Single secretory granules of live cells recruit syntaxin-1 and synaptosomal associated protein 25 (SNAP-25) in large copy numbers. *Proc Natl Acad Sci USA* 107:20810–20815.
16. Lang T, Margittai M, Hölzler H, Jahn R (2002) SNAREs in native plasma membranes are active and readily form core complexes with endogenous and exogenous SNAREs. *J Cell Biol* 158:751–760.
17. Kee Y, Lin RC, Hsu SC, Scheller RH (1995) Distinct domains of syntaxin are required for synaptic vesicle fusion complex formation and dissociation. *Neuron* 14:991–998.
18. Misura KM, Scheller RH, Weis WI (2000) Three-dimensional structure of the neuronal-Sec1-syntaxin 1a complex. *Nature* 404:355–362.
19. Hata Y, Slaughter CA, Südhof TC (1993) Synaptic vesicle fusion complex contains unc-18 homologue bound to syntaxin. *Nature* 366:347–351.
20. Voets T, et al. (2001) Munc18-1 promotes large dense-core vesicle docking. *Neuron* 31: 581–591.
21. Dulubova I, et al. (1999) A conformational switch in syntaxin during exocytosis: Role of munc18. *EMBO J* 18:4372–4382.
22. Graham ME, Barclay JW, Burgoyne RD (2004) Syntaxin/Munc18 interactions in the late events during vesicle fusion and release in exocytosis. *J Biol Chem* 279:32751–32760.
23. Takamori S, et al. (2006) Molecular anatomy of a trafficking organelle. *Cell* 127: 831–846.
24. Sankaranarayanan S, De Angelis D, Rothman JE, Ryan TA (2000) The use of pHluorins for optical measurements of presynaptic activity. *Biophys J* 79:2199–2208.
25. Perrais D, Kleppe IC, Taraska JW, Almers W (2004) Recapture after exocytosis causes differential retention of protein in granules of bovine chromaffin cells. *J Physiol* 560: 413–428.
26. Otto H, Hanson PI, Jahn R (1997) Assembly and disassembly of a ternary complex of synaptobrevin, syntaxin, and SNAP-25 in the membrane of synaptic vesicles. *Proc Natl Acad Sci USA* 94:6197–6201.
27. Barg S, et al. (2002) Delay between fusion pore opening and peptide release from large dense-core vesicles in neuroendocrine cells. *Neuron* 33:287–299.
28. Lang T, et al. (2000) Role of actin cortex in the subplasmalemmal transport of secretory granules in PC-12 cells. *Biophys J* 78:2863–2877.
29. Sieber JJ, Willig KI, Heintzmann R, Hell SW, Lang T (2006) The SNARE motif is essential for the formation of syntaxin clusters in the plasma membrane. *Biophys J* 90: 2843–2851.
30. Sieber JJ, et al. (2007) Anatomy and dynamics of a supramolecular membrane protein cluster. *Science* 317:1072–1076.
31. Pobbati AV, Stein A, Fasshauer D (2006) N- to C-terminal SNARE complex assembly promotes rapid membrane fusion. *Science* 313:673–676.
32. de Wit H, Cornelisse LN, Toonen RFG, Verhage M (2006) Docking of secretory vesicles is syntaxin-dependent. *PLoS One*, 10.1371/journal.pone.0000126.
33. Gerber SH, et al. (2008) Conformational switch of syntaxin-1 controls synaptic vesicle fusion. *Science* 321:1507–1510.
34. Hammarlund M, Watanabe S, Schuske K, Jorgensen EM (2008) CAPS and syntaxin dock dense core vesicles to the plasma membrane in neurons. *J Cell Biol* 180:483–491.
35. de Wit H, et al. (2009) Synaptotagmin-1 docks secretory vesicles to syntaxin-1/SNAP-25 acceptor complexes. *Cell* 138:935–946.
36. Chapman ER, Hanson PI, An S, Jahn R (1995) Ca2+ regulates the interaction between synaptotagmin and syntaxin 1. *J Biol Chem* 270:23667–23671.
37. Kee Y, Scheller RH (1996) Localization of synaptotagmin-binding domains on syntaxin. *J Neurosci* 16:1975–1981.
38. James DJ, Kowalchyk J, Daily N, Petrie M, Martin TF (2009) CAPS drives trans-SNARE complex formation and membrane fusion through syntaxin interactions. *Proc Natl Acad Sci USA* 106:17308–17313.
39. Shorter J, Beard MB, Seemann J, Dirac-Svejstrup AB, Warren G (2002) Sequential tethering of Golgins and catalysis of SNAREpin assembly by the vesicle-tethering protein p115. *J Cell Biol* 157(1):45–62.
40. McBride HM, et al. (1999) Oligomeric complexes link Rab5 effectors with NSF and drive membrane fusion via interactions between EEA1 and syntaxin 13. *Cell* 98: 377–386.
41. Lochner JE, et al. (1998) Real-time imaging of the axonal transport of granules containing a tissue plasminogen activator/green fluorescent protein hybrid. *Mol Biol Cell* 9:2463–2476.
42. An SJ, Almers W (2004) Tracking SNARE complex formation in live endocrine cells. *Science* 306:1042–1046.
43. Khakh BS, et al. (2001) Activation-dependent changes in receptor distribution and dendritic morphology in hippocampal neurons expressing P2X2-green fluorescent protein receptors. *Proc Natl Acad Sci USA* 98:5288–5293.
44. Shaner NC, et al. (2004) Improved monomeric red, orange and yellow fluorescent proteins derived from Discosoma sp. red fluorescent protein. *Nat Biotechnol* 22: 1567–1572.
45. Huang X, et al. (2001) Ca(2+) influx and cAMP elevation overcame botulinum toxin A but not tetanus toxin inhibition of insulin exocytosis. *Am J Physiol Cell Physiol* 281: C740–C750.
46. Watanabe N, Mitchison TJ (2002) Single-molecule speckle analysis of actin filament turnover in lamellipodia. *Science* 295:1083–1086.
47. Campbell RC (1989) *Statistics for Biologists* (Cambridge University Press, Cambridge) (Cambridgeshire).